Measurements on a Micromachined Silicon Gyroscope by Feedback Interferometry

V. Annovazzi-Lodi, *Senior Member, IEEE*, S. Merlo, *Member, IEEE*, and M. Norgia, *Member, IEEE*

***Abstract*—Feedback interferometry is a useful tool to characterize micromachined devices. In this paper, we consider a silicon vibrating gyroscope, in which the angular rotation is transduced into the vibration amplitude of a small suspended mass. Measurements of the mass displacement at submicrometer resolution are reported on a 400 × 400 μm sensor, using an 800-nm 20-mW laser diode. The resonance curves of the device have been determined for different values of pressure and other parameters, which allows us to tune the resonance frequency and maximize the Q factor. Hysteresis and other nonlinear phenomena on specific samples also have been detected. The proposed method provides a direct inspection tool and represents a practical alternative to the standard electrical measurements.**

***Index Terms*—Gyroscopes, microsensors, optical interferometry.**

I. Introduction

PROGRESS in micromachining technology has promoted the production of a wide range of sensors [1], which take advantage of the wafer-processing procedures developed by the electronics industry and exploit the good mechanical properties of silicon, such as a high fracture limit and a low density. Presently, a strong research effort is being addressed to the design of sensors for different physical parameters, which meet the requirements of industrial and consumer applications and are suitable for mass production at low cost.

Characterization measurements and diagnostics of such sensors often require a precise determination of displacement, speed, vibration amplitude, and other mechanical quantities. Unfortunately, standard methods are not always easy to implement on such small devices; on the other side, optical methods can often supply efficient solutions [2]–[4], and indeed scattering analysis and classical interferometry have still been proposed in such applications.

In this paper, we present an optical inspection method, based on feedback interferometry, which is suitable for fast and accurate characterization of vibrating micromachined devices, such as accelerometers and gyroscopes. This method has been especially developed to characterize a bare sensor, for which an electronic readout is not (yet) available on the chip; it represents a useful tool for measuring a device directly on the silicon wafer, before the scribing and packaging procedures.

Manuscript received February 8, 1999; revised January 3, 2000. Recommended by Technical Editor R. C. Luo. This work was supported by ST-Microelectronics and by CNR (Progetto Finalizzato Madess II).

The authors are with the Dipartimento di Elettronica, Universita' di Pavia, Pavia I-27100, Italy (e-mail: v.annovazzi@ele.unipv.it).

Publisher Item Identifier S 1083-4435(01)02720-X.

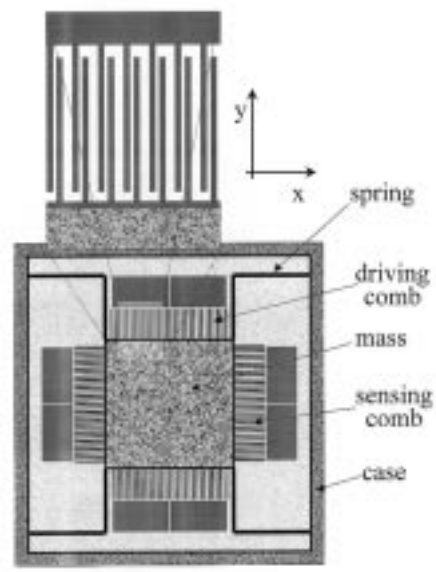

Fig. 1. Schematic layout of the vibrating mass gyroscope. Part of the capacitor comb for the gyro driving has been expanded.

II. Micromachined Gyroscope

As a practical case, we report on the characterization of silicon micromachined gyroscopes for automotive navigation and robotics.

These devices [4]–[10] are based on the Coriolis force acting on a vibrating mass upon rotation. A typical schematic layout is reported in Fig. 1.

The sensor consists of a laminar mass m (10^{-9}–10^{-8} kg weight, 200–600-μm side) suspended in the horizontal plane x-y by four laminar springs. The mass is forced to vibrate along the x-axis (driving axis) by an electrostatic force, which is generated by applying a periodic voltage to the capacitor comb highlighted in Fig. 1. In this structure, one plate of each capacitor is attached to the case of the gyro, and the other to the mass. Usually, some tens of capacitors are built along the relevant sides of the moving mass (the upper and lower sides in Fig. 1).

When the gyro rotates at angular velocity Ω around the vertical axis z (perpendicular to the xy-plane), the resulting Coriolis force $F_c = 2m\dot{x}\ \Omega$ causes a vibration along the y-axis (sensing axis), whose amplitude is proportional to Ω.

Thus, the angular rotation can be measured by reading the vibration amplitude along y. This can be done, as shown in Fig. 1, by building another capacitor comb along the y-axis, so that the vibration is transduced into a variation of capacity,

which is detected and amplified by a monolithic low-noise front-end built close to the sensor. (More advanced driving and sensing schemes, employing comb couples in a differential arrangement, are often used.)

If we apply to the driving axis a harmonic force $F = F_o \sin \omega t$, the displacements on the x- and y-axis are also harmonic at the same frequency. At the common resonance of both axes $\omega = (K/m)^{1/2}$, where K is the equivalent spring constant, the vibration amplitude is maximized and amounts to $X_d = Q_x F_o/K$ on the driving axis and to $Y_s = Q_y F_c/K$ on the sensing axis, where Q_x and Q_y are the quality factors [8].

For convenience, it is customary to drive the gyro by a square wave instead of a sinosoid. However, since the quality factors of the resonances are high by design, the mechanical structure provides filtering of high-order harmonics, and the system behavior is not strongly affected by the wave shape. Typical values of $f = \omega/(2\pi)$ are from 5 to 50 KHz, while X_d ranges from 0.5 to 5 μm and Y_s from 10 pm to 100 nm.

For design optimization, it is important to monitor the resonance curves of both axes as functions of the applied force and of other parameters. These measurements are aimed at implementing a functional matching of the x -and y-resonance frequencies (which are slightly different in a real gyro) and at increasing the Q factors. Both points are important to maximize responsivity [8]. From the resonance curves, one can also identify nonlinear or parasitic phenomena such as hysteresis of the mass displacement.

The typical readout scheme for capacitive sensors represents a method to perform such measurement. In our case, since we are driving and measuring the same axis, the driving signal should be applied only to one capacitor array of the axis under measure (e.g., the upper comb in Fig. 1 for the driving axis) while the other (the lower comb in Fig. 1) is used to transduce the mass vibration. Usually, the varying capacitance of such a comb is included in a voltage divider, which is fed by a high-frequency (1–10 MHz) carrier. Due to the mass inertia, the carrier does not contribute to vibration. However, the signal at the output of the divider, read by a high impedance amplifier, contains the frequency-translated and amplified response of the gyro to the driving waveform; thus the resonance curve can be observed on a spectrum analyzer simply by frequency sweeping the driving signal.

Alternatively, as explained in [11], the carrier can be applied directly between the moving mass and the electrical ground. In this case, a signal equivalent to that of the previous scheme is supplied by a transimpedance amplifier connected to the output comb.

Since they are suitable for implementation directly on the chip, such electrical schemes represent the most viable solution for the readout of a complete sensing device. However, they do not perform equally well on a bare sensor, where the output signal is reduced due to the stray capacitance of the connecting wires and of the external front end, which can be an order of magnitude higher than the whole capacitance of the combs (typically 0.1–0.5 pF [8]). Also, with some devices, such as our gyros, spurious beating between the driving signal and the carrier can mask the sensor response. Finally, since they require to modify the driving scheme, such electrical techniques do not measure the sensor in standard operating conditions.

An alternative solution, in principle, consists in the observation of the electrical impedance of the axis under measure. Basically, a sinusoidal voltage is applied to the relevant combs, and the input current is monitored while varying the frequency. By this method, one detects the mechanical resonance transduced into an electrical resonance, essentially as in a quartz resonator. Unfortunately, due again to the large stray capacitance, and because of the parasitic currents sunk by the semiconductor structure, this technique is often difficult to implement, especially on prototypes.

Obviously, a significant improvement should be expected by directly measuring the mechanical mass resonance by interferometry. However, classical interferometric schemes are not easy to implement in our case for different reasons. First, the vertical faces of the mass (in the planes xz and yz) are hidden by the case and/or silicon frame and cannot be reached by a laser beam. Second, the mass surface does not represent a good optical surface, since it is rough, and usually holed, both to remove the sacrificial layer and to reduce air damping. Finally, the setup must allow measurements inside a vacuum chamber, since for the design of the gyro it is important to determine Q as a function of pressure.

Though suitable tricks can be envisaged to implement, for example, a classical Michelson scheme, feedback interferometry provides a more efficient solution to our problem.

III. Measurements

Feedback interferometry [12], [13] is an interesting alternative to the classical interferometric techniques. A specific advantage is that it requires no external optics, other than a collimator or a focusing lens, which results in a simple and compact experimental setup. Also, it can operate with a very low backward signal from the target, it does not require accurate alignment and wavefront matching, and it works even on a diffusive surface.

Our experimental setup is shown in Fig. 2. The gyroscope was positioned in a glass vacuum chamber, on a suitable holder, at an angle $\alpha = 20°$ with respect to the laser beam. The laser/target distance was of about 40 cm. Feedback interferometry is based on the amplitude and frequency modulations arising on the laser oscillation when a small fraction P_j of the power P_0 emitted by a laser source is diffused, or reflected back, toward the laser itself by the target.

Different regimes have been described for weak to strong injection levels P_j/P_0 [12], [14], spanning from low-index AM and FM modulation, to strong perturbations and chaos.

Various schemes have been proposed for interferometric measurements based on weak-to-moderate injection. The current output signal from a photodiode at the rear laser mirror (PD2), or at a detector fed by a part of the output beam (PD1), has the form [13]

$$I = I_o + I_{\max} \cos(\omega_f \tau). \tag{1}$$

In this equation, I_o is proportional to the laser output power, $I_{\max}$ is proportional to the injected power, τ is the roundtrip

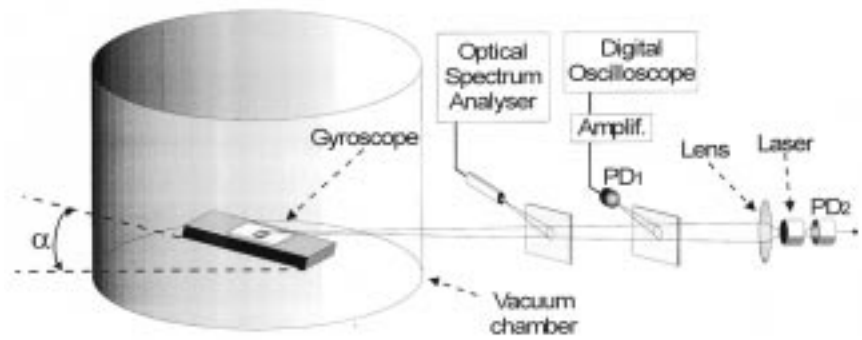

Fig. 2. Experimental setup for the interferometric measurements on the gyro.

time in the external cavity (defined by the laser output mirror and the target), and ω_f is the angular frequency of the laser with the external cavity, which can be calculated from the condition of zero round-trip phase change.

As explained elsewhere [12], [13], by working at moderate injection levels $(P_j/P_0 > 10^{-6})$, it is possible to derive from the photodetected signal (1) the absolute displacement of the target with its sign; by suitable processing, one can also reconstruct the target movement.

In the following, however, we will focus on the weak injection regime $(P_j/P_0 < 10^{-6})$ [12], [14], [15], which is observed with the low-level backward signals provided by our diffusing target at a small angle α. In this regime, the frequency modulation in (1) is weak. Thus, ω_f is virtually equal to the unperturbed laser frequency $\omega_o = 2c\pi/\lambda$, where λ is the laser wavelength and c is the speed of light, and the expression of the photodetected current I can be simplified to

$$I(t) = I_o + I_{\max}\cos\omega_o\tau = I_o + I_{\max}\cos[(4\pi/\lambda)s(t)] \quad (2)$$

where $s(t)$ is the component of the target displacement along the direction of the laser beam. It follows that for weak injection, the target displacement relative to a reference position can be obtained simply by fringe counting, e.g., by detecting the zero-crossings of the interferometric signal $I(t) - I_o$.

Our measurements were made by using an SDL 5400 infrared laser diode at 800-nm emission wavelength. This source was selected because it exhibits a stable monomode spectrum under different injection conditions. While its maximum output power is $P_0 = 100$ mW, the source was operated at $P_0 = 20$ mW (10% over its threshold current), as a tradeoff between the relative modulation amplitude (which is maximum at threshold) and the signal amplitude $I_{\max}$, which is proportional to P_0.

It must be pointed out that signal fading due to the diffusion regime [16] was just a minor problem in our setup. Indeed, the coherence region for a Gaussian diffuser in the speckle-pattern regime has a length

$$L_1 = (16\sqrt{3}/\pi)\lambda(L/D)^2 \quad (3)$$

at a distance L along the beam and a width

$$L_2 = (4/\pi)\lambda(L/D) \quad (4)$$

in the transverse direction, where D is the diameter of the laser spot on the target (or its projection for non normal incidence).

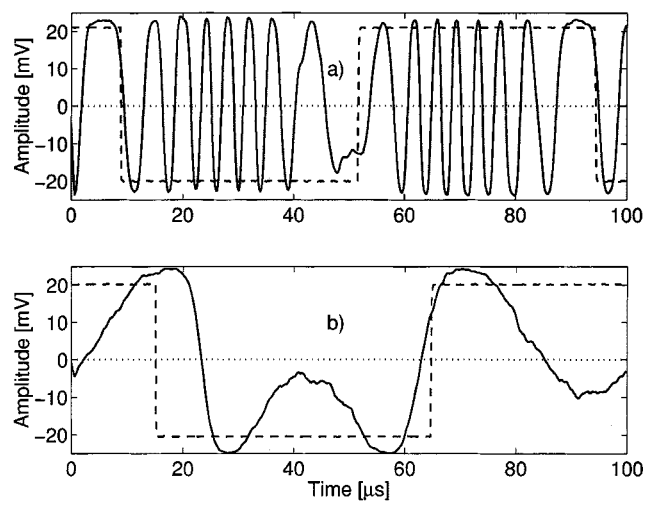

Fig. 3. Typical interferometric signals at atmospheric pressure at the output photodiode PD1: (a) at resonance ($f = 11.69$ kHz) and (b) out of resonance ($f = 12.61$ kHz).

With our parameter values, L_1 is in excess of 1 m, while L_2 is in the range 1–5 mm. On the other side, the target movement was limited within a few micrometers. In practice, we had only to maximize occasionally the interferometric signal by slightly adjusting the source position.

Also, it is interesting to observe that an optical grade window was not required for the vacuum chamber. Indeed, our experiments have been made through a standard glass bell, simply by focussing or collimating the beam on the target, and avoiding to work orthogonally to the surface to reduce disturbing reflections. The beam translation was compensated for by moving the source.

Our measurements were performed on different samples of a 400-μm-side gyro, made by surface micromachining with epitaxial growth. The moving mass was 10-μm thick, and its weight was 2.5 μg. The diagrams reported in Figs. 2–5 are pertinent to the same device for easy comparison.

Typical measured plots of the varying component of $I(t)$ are shown in Fig. 3(a) and (b) for the driving axis. In each plot, the forcing square wave is also shown to highlight its timing relative to the interferometric signal.

From these diagrams, it can be appreciated that the mass vibrates synchronously with the high and low levels of the square wave. The phase inversion at the square wave edges is also evident. The maximum displacement in Fig. 3(a) (i.e., at resonance)

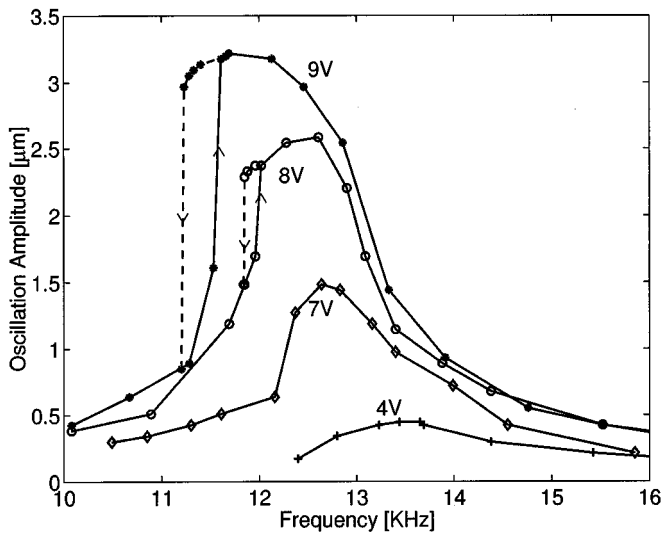

Fig. 4. Vibration amplitude versus frequency for the driving axis of the micromachined gyro at standard atmospheric pressure for different values of the forcing electrical signal. The typical hysteresis diagram of a "soft" spring oscillator has been found.

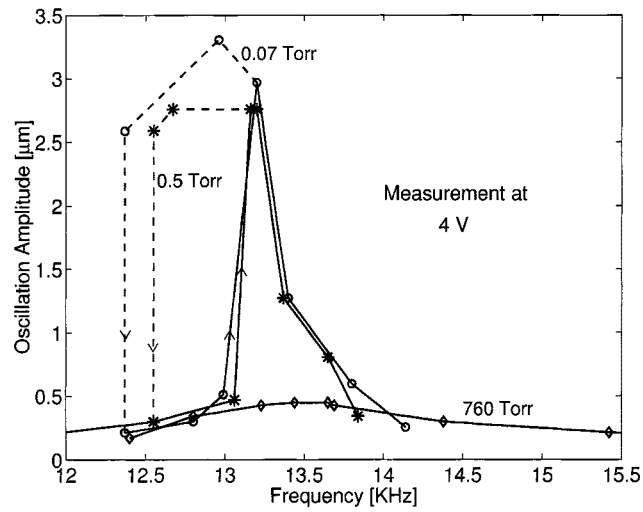

Fig. 5. Vibration amplitude versus frequency for the driving axis of a micromachined gyro at different pressures for a 4-V forcing electrical signal.

is of about seven fringes, corresponding to a maximum elongation $S_{\max} = 7 \times 400\,\text{nm} = 2.8\ \mu$m, or to a true vibration amplitude $S = S_{\max}/\cos\alpha = 3\ \mu$m.

The diagrams of Fig. 3 were taken at a digital oscilloscope, after amplification of $I(t)$ by a standard high-pass transimpedance scheme. By averaging on 8–64 periods of the square wave, the effects of the slow ambient vibrations coupled to the mechanical setup were strongly reduced. This provided a very good signal-to-noise ratio, which allowed us to appreciate even a fraction of a fringe.

Fig. 4 shows the resonance curves of the driving axis at atmospheric pressure for different amplitudes of the forcing electrical signal. These diagrams have been drawn after measurements such as those shown in Fig. 3. It is interesting to observe the hysteresis on the low-frequency side of the resonance curve. This effect increases for stronger driving and has been explained in [17]; it is typical of a "soft" mechanical oscillator, i.e., an oscillator having a spring for which the restoring force increases less than linearly with displacement. A similar effect has been reported in [18].

Another interesting finding is the Q_x reduction arising when, at excessive driving amplitude, the plates of the capacitors come in touch. In this situation, the mass elongation at frequencies at or near the resonance tends to saturate at a value equal to the distance between the two adjacent combs. Thus, the maximum of the resonance curve is somewhat flattened, and the Q factor is reduced. This (incipient) regime can be observed by comparing the first curve in Fig. 4, taken at 9-V driving, with the lower one, taken at 8-V driving. The effect would be more evident at higher driving; unfortunately, strong overdriving would result in permanent damage of the gyro.

Resonance curves are also shown in Fig. 5 for different values of pressure. From these plots, and from other measurements at different driving amplitudes, the practically obtainable value of the quality factor can be found, as well as the required vacuum level for the gyro operation, which is an important information for the package design.

For our gyroscope, it has been found that Q_x increases rapidly from a bare value of four to eight at atmospheric pressure to more than 50 at 0.5 torr and then rapidly saturates. This behavior is due to the transition from squeeze damping (due to the forced air flow between the minute mechanical parts of the sensor) to the lower viscous damping for reduced air density. Though this value is lower than usually reported in literature for similar devices, it has been confirmed by the electrical measurements and is compatible with a device that is still under development. When measuring commercial devices (such as accelerometers) at low pressure, our method allowed us to detect Q values in excess of 1000.

Also, note in Fig. 5 that the hysteresis increases at lower pressure (i.e., at lower damping), as expected.

Other plots, similar to those of Figs. 3–5, have been obtained for the sensing axis, thus getting a complete mechanical characterization of the gyroscope for design and diagnostic purposes.

With our setup, the measurement resolution can be estimated in about one-eighth of the optical wavelength (100 nm in our case). The minimum detectable signal is of the same order. Both figures were limited by the operator's ability to analyze the interferometric signal below a single fringe, by simply observing $I(t)$ at a digital storage oscilloscope. Better results could be obtained by analog or digital electronic processing, or by waveform extraction by a suitable software routine.

The measurement uncertainty was principally due to ambient vibrations, which are detected as spurious signals by the interferometer. Fortunately, as already stated, this effect can be strongly reduced by averaging (see Fig. 3) so that in Figs. 4 and 5, the error on the experimental points is of the order of 25–50 nm.

This figures are somewhat better than those obtained by the standard electrical method in our experimental conditions. For comparison, in Fig. 6, we report the resonance curve of a similar device, as obtained by feedback interferometry and by the electrical scheme reported in [11] with a carrier frequency of 2 MHz.

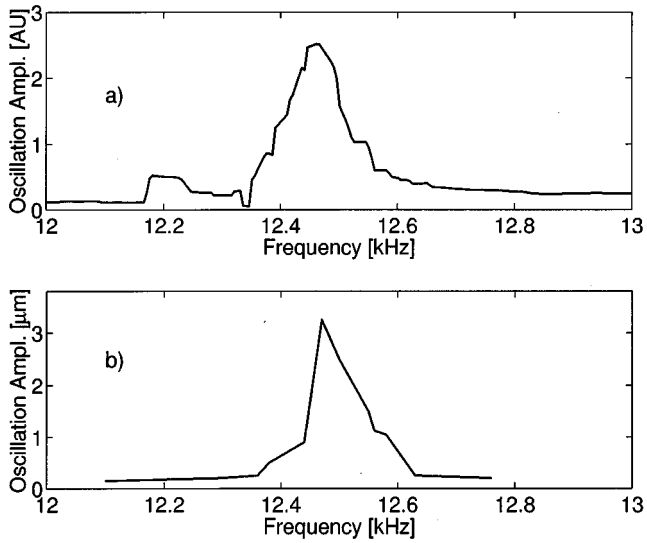

Fig. 6. Resonance curve of a gyroscope measured at 0.6 torr by (a) standard electrical method and (b) feedback interferometry.

The results shown in Fig. 6 are consistent. However, the resonance curve meausured by the electrical method, and observed at a spectrum analyzer, was superposed to a much larger pedestal, i.e., to a spurious beating between the driving signal and the carrier. This disturbance, probably caused by nonlinear superposition of the two applied waveforms on the silicon structure, was frequency dependent and resulted in a rather difficult measurement of the resonance curve for low Q, where the response is very smooth. On the other side, we could easily measure the resonance interferometrically even at atmosferic pressure.

Another advantage of the optical method was that only two wires (for the driving signal) had to be connected to the chip and passed through the vacuum bell. More important, no critical cabling to detect the output signal was required.

Finally, it is interesting to observe that since the optical beam can be focussed on the target, feedback interferometry can be applied to very small sensor elements without significant signal reduction. The spatial resolution with our setup was on the order of 5–10 μm. However, with a relatively large target such as a gyro, a wider beam was usually employed to speed up the alignment procedures.

IV. Conclusion

In conclusion, feedback interferometry has proven to be an effective tool for the characterization of silicon micromachined gyros. This technique can be used for other micromachined mechanical sensors, such as accelerometers. With respect to standard interferometry, this method is much less sensitive to the wavefront distorsion due to scattering from the target or the medium. It does not require external optics other than a focusing lens and performs well even at large incidence angles.

With respect to standard electrical measurements, feedback interferometry provides a direct and easier way to characterize a bare sensor; it provides *in situ* noninvasive monitoring of the device, since it directly measures the mass vibration and does not require to modify the standard electrical driving method.

Acknowledgment

The authors wish to express their sincere appreciation to Prof. S. Donati for his guidance throughout the course of their scientific activity.

References

[1] *Proc. SPIEMicromachined Devices and Components III*, vol. 3224, K. Chau and P. J. French, Eds, 1997.
[2] S. C. Holswade and F. M. Dickey, "Optical measurement of micromachine engine performance," in *Proc. SPIE Micromachined Devices and Components III*, vol. 3224, 1997, pp. 131–140.
[3] K. Tanaka, Y. Mochida, M. Sugimoto, K. Moriya, T. Hasegawa, K. Atsuchi, and K. Ohwada, "A micromachined vibrating gyroscope," *Sensors & Actuators*, vol. A50, pp. 111–115, 1995.
[4] Y. Mochida, M. Tamura, and K. Phwada, "A micromachined vibrating rate gyroscope with independent beams for the drive and detection modes," in *Proc. IEEE MicroElectromechanical Systems Workshop*, Orlando, FL, Jan. 1999, pp. 618–623.
[5] R. Voss, "Silicon micromachined vibrating gyroscopes," in *Proc. SPIE Micromachined Devices and Components III*, vol. 3224, 1997, pp. 62–73.
[6] *Proc. Symp. Gyro Technology 1997*, H. Sorg, Ed., Stuttgart, Germany, Sept. 16–17, 1997.
[7] K. Y. Park, C. W. Lee, Y. S. Oh, and Y. H. Cho, "Laterally oscillated and force-balanced micro vibratory rate gyroscope supported by fish-hook-shaped springs," *Sensors Actuators A*, vol. A-64, pp. 69–76, 1998.
[8] M. S. Kranz and G. K. Fedder, "Micromechanical vibratory rate gyroscopes fabricated in conventional CMOS," in Proc. Symp. Gyro Technology 1997, Stuttgart, Germany, Sept. 16–17, 1997, Paper 3.
[9] N. Barbour and G. Schmidt, "Inertial sensor technology trends," *Proc. IEEE 1998 Workshop Autonomous Underwater Vehicles*, pp. 55–62, Aug. 20–21, 1998.
[10] G. Fetzer *et al.*, "Yaw rate sensor in silicon micromachining technology for automotive applications," in *Proc. Symp. Gyro Technology 1997*, paper 8, Stuttgart, Germany, Sept. 15/16, 1998.
[11] W. C. Tang, T. C. H. Nguyen, M. W. Judy, and R. T. Howe, "Electrostatic-comb drive of lateral polysilicon resonator," *Sensors Actuators*, vol. A21, pp. 328–331, 1990.
[12] S. Donati, G. Giuliani, and S. Merlo, "Laser diode feedback interferometer for measurement of displacement without ambiguity," *IEEE J. Quantum Electron.*, vol. 31, pp. 113–119, 1995.
[13] S. Donati and S. Merlo, "Applications of diode laser feedback interferometry," *J. Opt.*, vol. 29, pp. 156–161, 1998.
[14] K. Peterman, "External optical feedback phenomena in semiconductor lasers," *IEEE J. Select. Topics Quantum Electron.*, vol. 1, pp. 480–489, 1995.
[15] M. A. Hauptmann, K. T. V. Grattan, A. W. Palmer, H. Fritsch, R. Lucklum, and P. R. Hauptmann, "Silicon resonator sensor system using self-mixing interferometry," *Sensors Actuators*, vol. A55, pp. 71–77, 1996.
[16] S. Donati, S. Merlo, and F. Micolano, "Feedback interferometry with semiconductor laser for high resolution displacement sensing," in *Proc. SPIE Micro-Optical Technologies for Measurement, Sensors, and Microsystems*, vol. 2783, 1996, pp. 203–210.
[17] H. J. Pain, *The Physics of Vibrations and Waves*, London, U.K.: Wiley, 1968, ch. 11.
[18] J. D. Zook, D. W. Burns, H. Gukel, J. J. Sniegowski, R. L. Engelstad, and Z. Feng, "Characteristics of polysilicon resonant microbeams," *Sensors Actuators*, vol. A35, pp. 51–59, 1992.

V. Annovazzi-Lodi (M'89–SM'99) was born in Novara, Italy, on November 7, 1955. He received the degree in electronic engineering from the University of Pavia, Pavia, Italy, in 1979.

Since 1979, he has been with the Department of Electronics, University of Pavia, working in the fields of electronics and electrooptics. His main research interests include injection phenomena and chaos in oscillators and lasers, electrical fiber sensors, the fiber gyroscope, passive fiber components for telecommunications and sensing, optical amplifiers, trasmission via diffused infrared radiation, and micromechanical systems. In 1983, he became a Staff Researcher with the Department of Electronics, University of Pavia, and in 1992, he became an Associate Professor. He is the author of more than 70 papers and is the holder of 4 patents.

Dr. Annovazzi-Lodi is a member of AEI.

S. Merlo (M'01) was born in Pavia, Italy, in 1962. She received the degree *(cum laude)* in electronic engineering from the University of Pavia in 1987, the M.S.E. degree in bioengineering from the University of Washington, Seattle, in 1989, and the Ph.D. degree in electronic engineering from the University of Pavia.

Since 1993, she has been an Assistant Professor at the Department of Electronics, University of Pavia. Her main research interests include fiber-optic passive components and sensors, optical amplifiers, laser interferometry, and microelectromechanical systems. She has received three patents and is the author of approximately 40 papers.

Dr. Merlo is a member of AEI. She received a Rotary Foundation Graduate Scholarship to study at the University of Washington.

M. Norgia (M'98) was born in Omegna, Italy, in 1972. He graduated in electronics engineering i 1996 from the University of Pavia, Pavia, Italy, and where he is currently working toward the Ph.D. degree in electronics engineering and computer science.

His dissertation was on noise in optical amplifiers. His main research interests are noise in optical amplifiers and interferometry.